In-silico folding of a three helix protein and characterization of its free-energy landscape in an all-atom forcefield

T. Herges[1] and W. Wenzel[1]

[1]*Forschungszentrum Karlsruhe, Institut für Nanotechnologie, 76021 Karlsruhe, Germany*
(Dated: June 18, 2003)

We report the reproducible first-principles folding of the 40 amino acid, three-helix headpiece of the HIV accessory protein in a recently developed all-atom free-energy forcefield. Six of twenty simulations using an adapted basin-hopping method converged to better than 3 Å backbone RMS deviation to the experimental structure. Using over 60,000 low-energy conformations of this protein, we constructed a decoy tree that completely characterizes its folding funnel.

Available genomic and sequence information for proteins contains a wealth of biomedical information that becomes accessible when translated into three-dimensional structure [1]. While theoretical models for protein structure prediction [2, 3] that partially rely on experimental information have shown consistent progress[4], the assessment of de-novo strategies that rely on sequence information alone has been much less favorable [5]. The development of such techniques, in particular of transferable first-principle all-atom folding methods, would significantly benefit the understanding of protein families where little experimental information is available, the prediction of novel folds as well as the investigation of protein association and dynamics which are presently difficult to probe experimentally. Recent progress for small peptides [3, 6, 7, 8] documents both the feasibility of this approach as well as its limitations [9, 10], in particualr those associated with the direct simulation of the folding process through molecular dynamics [11].

Overwhelming experimental evidence supports the thermodynamic hypothesis [12] that many proteins are in thermodynamic equilibrium with their environment: their native state thus corresponds to the global minimum of their free energy landscape [13]. The free energy of the system is accessible either indirectly by explicit ensemble averaging of the combined internal energy of protein and solvent, or directly in a free-energy forcefield where an implicit solvation model approximates direct interactions with the solvent as well as most of the entropic contributions. We developed an all-atom protein forcefield (PFF01) [8, 14, 15] with an area-based implicit solvent model that approximates the free energy of peptide conformations in the natural solvent. Using a rational decoy approach this forcefield was optimized to correctly predict the native structure of the 36-amino acid headgroup of villin [9, 10, 11]. Without further parameter adjustment we then simulated the structurally conserved 40 amino-acid headpiece of the autonomously folding HIV accessory protein (1F4I-40) [16] with a modified basin hopping technique [17, 18]. Out of twenty simulations the five energetically lowest correctly reproduced the NMR structure of this three-helix protein with a backbone RMS deviation of less than 3 Å. The combination of decoy based model development for the free energy with efficient stochastic optimization methods suggests a viable route for protein structure prediction at the all atom level with present day computational resources.

Model: We have recently developed an all-atom protein forcefield (PFF01), which was used to reproducibly fold the 20 amino acid trp-cage protein [8]. PFF01 [15] comprises an atomically resolved electrostatic model with group specific dielectric constants and a Lennard Jones parameterization that was adapted to the experimental distance distributions from crystal structures of 138 proteins [19]. Interaction with the fictitious solvent are modeled in a simple solvent accessible surface approach [20], where the solvation free-energies per unit surface were fitted to the enthalpies of solvation of the Gly-X-Gly series of peptides [21]. The only low-energy degrees of freedom available to the peptide during the folding process are rotations of the dihedral angles of the backbone and the sidechains, these are the only moves considered during the simulation. There are two move-classes, small random rotations about a single angle and library moves, which set a particular backbone dihedral to a permitted value in the Ramachandran plot.

If an accurate model for the free energy of the protein in its environment is available, stochastic optimization methods can be used to locate the global optimum of the free-energy landscape orders of magnitude faster than traditional simulation techniques. We adapted the basin hopping technique [17] (BHT) for protein simulations by replacing a single minimization step with a simulated annealing run [22] with self-adapting cooling cycle and length. At the end of one annealing step the new conformation was accepted if its energy difference to the current configuration was no higher than a given threshold energy ε_T, an approach recently proven optimal for certain optimization problems [23]. Each simulation was performed in three separate steps: First we used a high temperature bracket of 800/300 K (ε_T =15 K) for the annealing window and reduced the strength of the solvent

Name	RMSB	Energy	Secondary Structure Content
N	0.00		ccHHHHHHHHHclcbHHHHHHHHHHHclcccHHHHHHHHHc
D01	2.34	-119.54	cHHHHHHHHHHHlcbcHHHHHHHHHHHHbHHHHHHHHHHc
D02	2.41	-117.52	cHHHHHHHHHHHHlcbHHHHHHHHHHHHHbHHHHHHHHHHc
D03	2.76	-116.25	cHHHHHHHHHHHHlcbHHHHHHHHHHHHHbHHHHHHHHHHc
D04	2.40	-115.85	cHHHHHHHHHHHHlbbHHHHHHHHHHHHHbHHHHHHHHHHc
D05	2.43	-114.67	cHHHHHHHHHHHHlcbHHHHHHHHHHHHcbHHHHHHHHHHHc
D06	6.48	-114.06	cHHHHHHHHHHHHcccbHHHHHHHHHHHHbHHHHHHHHHHc
D07	2.57	-113.65	cHHHHHHHHHHHHlbbcHHHHHHHHHHHHbHHHHHHHHHHc
D08	4.61	-107.72	cHHHHHHHHHHcclccHHHHHHHHHHHHHlclHHHHHHHHc
D09	4.14	-106.29	cHHHHHHHHHHHHcbcbHHHHHHHHHHbblcHHHHHHHHHc
D10	5.92	-103.88	cHHHHHHHHHHHHlcHHHHHHHHHHbcbcclbHHHHHHHHHc

TABLE I: Table of the 10 lowest energy decoys (of 20, remainder available by request from the authors) with backbone RMS deviation to the NMR structure and secondary structure content. The first row designates the secondary structure content of the NMR structure.

terms in the forcefield by 20%. The second step started from the final configurations of the first run, used the same annealing window but the full solvent interactions. In the third step the resulting structures were further annealed in a low temperature bracket of $600/3$ K (ε_T=1K). Within each annealing run the temperature was geometrically decreased, also the number of steps per annealing run was gradually increased to ensure better convergence. In total each simulation comprised 10^7 energy evaluations with a computational effort roughly corresponding to a 10 ns MD simulation (in vacuum with 1 fs timestep). After this time no significant energy fluctuations occurred in the simulations, indicating that each had settled into a metastable configuration.

Results: Using PFF01 we performed 20 independent modified basin hopping simulations of the structurally conserved 40 amino-acid headpiece of the HIV accessory protein (pdb-code 1F4I, sequence: QEKEAIERLK AL-GFEESLVI QAYFACEKNE NLAANFLLSQ). The best structures found in each run were ranked according to their energy and the backbone RMS deviation (RMSB) to the NMR structure was computed. Table (I) demonstrates that the five lowest structures had to good accuracy converged to the NMR structure of the protein. The first non-native decoy appears in position six, with an energy deviation of 5 kcal/mol (in our model) and a significant RMSB deviation. The table demonstrates that all low-energy structures have essentially the same secondary structure, i.e. position and length of the helices are always correctly predicted, even if the protein did not fold correctly. The degree of secondary structure content and similarity decreases for the decoys with higher energy (data not shown) in good correlation with their energy. From the standpoint of the optimization approach (but not necessarily for the physical folding scenario) this suggests that successful folding requires the formation of the correct secondary structure content as a prerequisite.

The good agreement between the folded and the experimental structure is also evident from Figure (1), which shows the secondary structure alignment of the native and the folded conformations. The good physical alignment of the helices illustrates the importance of hydrophobic contacts to correctly fold this protein. An independent measure to assess the quality of these contacts is to compare the C_β-C_β distances (which correspond to the NOE constraints of the NMR experiments that determine tertiary structure) in the folded structure
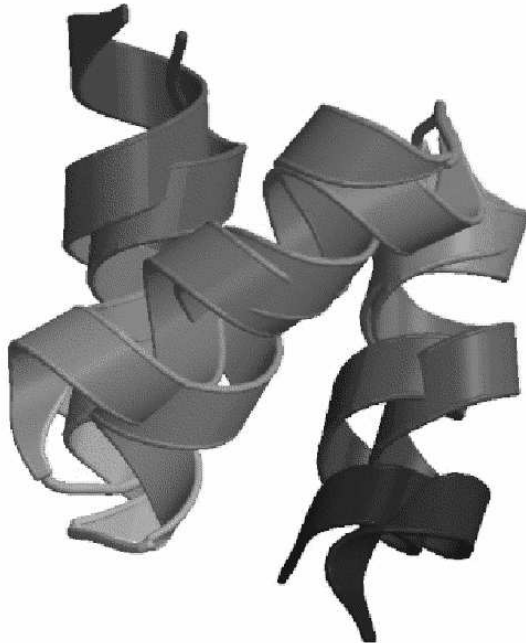

FIG. 1: Overlay of the secondary structure elements of the native configuration and the folded structure of 1F4I-40
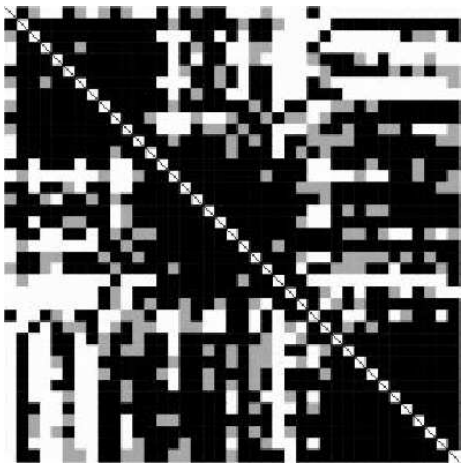
FIG. 2: Color coded C_β-C_β distance error map for the folded structure 1F4I in comparison to the NMR structure. Each square encodes the deviation between the C_β-C_β distance of two amino acids in the NMR to the C_β-C_β distance of the same amino acids in folded structure. Black (grey) squares indicate a deviation of less than 1.50 Å (2.25 Å). White squares indicate large deviations.

to those of the native structure. The color coded C_β-C_β distance in Figure (2) demonstrates a 66 % (80 %) coincidence of the C_β-C_β distance distances to within one (1.5) standard deviations of the experimental resolution. The dark diagonal block indicate intra-helical contacts, which are, perhaps not too surprisingly, resolved to very good accuracy. The off-diagonal dark blocks, however, indicate that also a large fraction of long range native contacts is reproduced correctly.

Starting from intermediate structures of the folding simulations we generated over 60,000 low-energy conformations (decoys). Decoys with a root mean square deviation of the backbone (RMSB) deviation of less than 3 Å were grouped into families with free energy brackets of 2 kcal/mol. We then resolved the topological hierarchy[18, 24] of the associated potential energy surface through the construction of a decoy tree (Figure (3)) that illustrates the low-energy structure of the free energy surface. Beginning from the best conformation, we draw a vertical line for each decoy family in this window. Moving upward in energy the number of decoys in each family grows almost exponentially in the low energy region which we can resolve well. As a result the diversity of each family grows until different families unite. Family membership is associative, i.e. as soon as two decoys in different branches have an RMSB deviation of less than 3 Å, all members of both families belong to one superfamily. Pictorially this representation results in an inverted tree-like structure that characterizes the topology of the metastable states of the free energy surface.

Trees with very short stems and many low-energy branches are characteristic of glassy potential energy surfaces, which are associated with Levinthals paradox [25, 26] in the context of protein folding. Well structured trees with few terminal branches suggest the existence of a folding funnel [13], consistent with the "new" paradigm for protein folding [27]. From this perspective the structure in Figure (3) this tree is indicative of the existence of a very broad folding funnel [13] with pronounced competing secondary metastable conformations, which are depicted as the non-native terminal minima of the tree. The discretization of the energy axis in intervals of 2 kcal/mol starting from the native conformation results in a smoothing of the free-energy surface. Each line in the figure corresponds to a family containing hundreds tothousands of structures, which are all associated with the same low-lying metastable conformation (the terminal point of the branch). Simulations trapped in such a metastable state must overcome a potential energy barrier of the order of the energy difference to the next highest branching point of the tree to visit another structure. The branching points of the tree were constructed only from structures of the decoy set and not through independent transition state search among the terminal structures. In addition, main-chain entropy is neglected in this analysis, which results in an overestimation of the barrier. Further investigations to more accurately determine the transition states are presently under way.

The lowest competing terminal branch (branch C), associated with decoy D06 in Table (I), is less than 5 kcal/mol above the best native decoy. Decoy D06 has comparable energy to competing decoys but much larger RMSB deviation and has few long-range native contacts. This structure (see Figure (4)) has also three helices of comparable length and sequence location, but differs from the native structure in the relative alignment of the
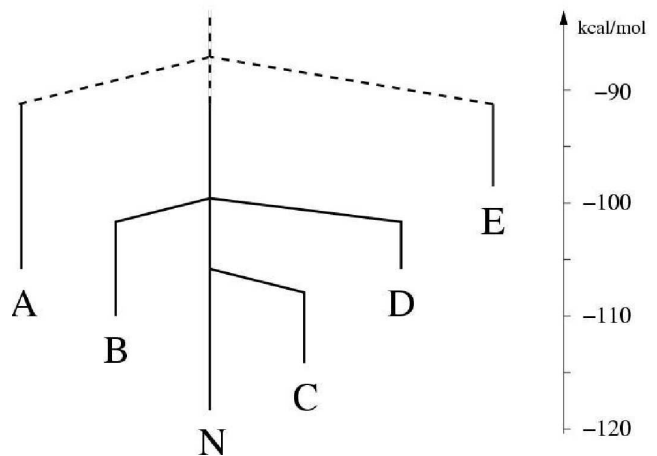

FIG. 3: Decoy tree of the low energy configurations of the 40 amino acid headpiece of th HIV accessory protein. The horizontal axis depicts the total energy the chart on the right the total number of decoys in the primary and secondary funnels.
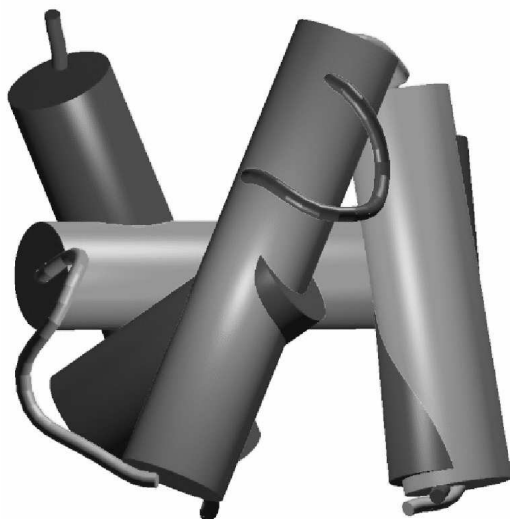
FIG. 4: Overlays of the secondary structure elements of the native (green) configuration and the lowest misfolded decoy (red) of 1F4I.

helices with respect to each. The RMSB deviation of the low-lying terminal structures to the NMR structures is large (i.e. comparable with the RMSB deviation to unfolded structures), indicating that conserved secondary structure elements, rather than distance constraints characterize the folding funnel. The low lying local minima are thus characterized by varying spatial arrangements of similar secondary structure elements, a property that is ill represented by either RMSB deviation or the number of native contacts.

Discussion: With this work we have demonstrated that accurate free-energy forcefields can predict the native structure of proteins with nontrivial tertiary structure with present day computational resources. This result represents an *in-silico* realization of the thirty year-old thermodynamic hypothesis that proteins are in thermodynamic equilibrium with the environment under physiological conditions [12]. Under this hypothesis, the native structure of the protein can be predicted using stochastic optimization methods orders of magnitude faster than by direct simulation. Our results demonstrate that the important influence of the solvent can be modeled with a relatively simple solvent accessible surface approach.

The analysis of the free energy surface supports the funnel paradigm of protein folding for a nontrivial protein with a significantly larger hydrophobic core than was previously possible. The relatively small number of terminal branches of the decoy tree offers the first glimpse on the experimentally inaccesible structure of the folding funnel. It suggest the exsitence of a broad folding funnel with well defined secondary metastable states which may constitute important folding intermediates. The free energy optimization approach used here permitted the characterization of these low-lying states, which surpris-

ingly share very similar secondary structure with the native configurations. Investigations of other proteins must show, whether this pattern persist also for other proteins.

It should be noted that the success of the optimization approach depends strongly on the ability of the optimization technique to differentiate between the low-lying minima of the FES *in a realistic forcefield.* The performance of optimization methods is often strongly problem dependent, but with 1F4I, 1VII and 1L2Y three nontrivial model systems exist on which different optimization methods can be evaluated. The decoy sets generated and insights regarding low-lying metastable states can also serve as a test-bed for the development of coarse-grained protein models. PFF01 is presently be validated for other peptides and proteins and rationally evolved to correctly predict the structure of larger fold families.

[1] D. Baker and A. Sali, Science **294**, 93 (2001).
[2] J. Schonbrunn, W. J. Wedemeyer, and D. Baker, Curr. Op. Struc. Biol. **12**, 348 (2002).
[3] A. Liwo, P. Arlukowicz, C. Czaplewski, S. Oldizeij, J. Pillardy, and H. Scheraga, Proc. Natl. Acad. ¡Sci.(USA) **99**, 1937 (2002).
[4] J. Moult, K. Fidelis, A. Zemia, and T. Hubbard, Proteins **45**, 2 (2001).
[5] R. Bonneau, J. Tsui, I. Ruczinski, D. Chivian, C. M. E. Strauss, and D. Baker, Proteins **45**, 119 (2001).
[6] C. D. Snow, H. Nguyen, V. S. Panda, and M. Gruebele, Nature **420**, 102 (2002).
[7] C. Simmerling, B. Strockbine, and A. Roitberg, J. Am. Chem. Soc. **124**, 11258 (2002).
[8] A. Schug, T. Herges, and W. Wenzel, Phys. Rev. Letters **91**, 158102 (2003).
[9] H. Hansmann, Phys. Rev. Letters **88**, 068105 (2002).
[10] C. Lin, C. Hu, and U. Hansmann, Proteins **53**, 436 (2003).
[11] Y. Duan and P. A. Kollman, Science **282**, 740 (1998).
[12] C. B. Anfinsen, Science **181**, 223 (1973).
[13] J. N. Onuchic, Z. Luthey-Schulten, and P. G. Wolynes, Annu. Rev. Phys. Chem. **48**, 545 (1997).
[14] A. Schug, H. Merlitz, and W. Wenzel, Nanotechnology **14**, 1161 (2003).
[15] T. Herges and W. Wenzel, *Development of an all-atom forcefield for teriatry structure prediction of helical proteins*, (submitted).
[16] E. S. Withers-Ward, T. Mueller, I. Chen, and J. Feigon, Biochemistry **39**, 14103 (2000), 1F4I.
[17] A. Nayeem, J. Vila, and H. Scheraga, J. Comp. Chem. **12**(5), 594 (1991).
[18] J. P. Doyle and D. Wales, J.Chem.Phys. **105**, 8428 (1996).
[19] R. Abagyan and M. Totrov, J. Molec. Biol. **235**, 983

(1994).

[20] D. Eisenberg and A. D. McLachlan, Nature **319**, 199 (1986).

[21] K. A. Sharp, A. Nicholls, R. Friedman, and B. Honig, Biochemistry **30**, 9686 (1991).

[22] S. Kirkpatrick, C. Gelatt, and M. Vecchi, Science **220**, 671 (1983).

[23] J. Schneider, I. Morgenstern, and J. Singer, Phys. Rev. E **58**, 5085 (1998).

[24] C. L. Brooks, J. N. Onuchic, and D. J. Wales, Science **293**, 612 (2001).

[25] C. Levinthal, J. Chim. Phys. **65**, 44 (1968).

[26] B. Honig, JMB **293**, 283 (1999).

[27] A. Šali, E. Shakhnovich, and M. Karplus, Nature **369**, 248 (1994).